Industrial Crops & Products 211 (2024) 118217

Contents lists available at ScienceDirect

Industrial Crops & Products

journal homepage: www.elsevier.com/locate/indcrop

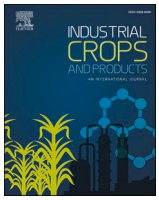

Chemical composition and structural features of cellolignin from steam explosion followed by enzymatic hydrolysis of *Eucalyptus globulus* bark

Sandra Magina [a], Susana Marques [b], Francisco Gírio [b], Ana Lourenço [c], Ana Barros-Timmons [a], Dmitry V. Evtuguin [a,*]

[a] CICECO-Aveiro Institute of Materials and Department of Chemistry, University of Aveiro, 3810-193 Aveiro, Portugal
[b] LNEG - Laboratório Nacional de Energia e Geologia I.P., Unidade de Bioenergia e Biorrefinarias, Estrada do Paço do Lumiar 22, Edifício F, 1649-038 Lisbon, Portugal
[c] Forest Research Center, School of Agriculture, University of Lisbon, Tapada da Ajuda, 1349-017 Lisboa, Portugal

ARTICLE INFO

Keywords:
Eucalyptus globulus bark
Steam explosion
Enzymatic hydrolysis
Lignin
Cellulose
Tannins

ABSTRACT

Bark is one of the main wastes of the chemical and mechanical processing of *Eucalyptus globulus* wood. The proposed biochemical processing of bark via saccharification pathway involves steam explosion (SE) pretreatment (severity factor log R_0 of 4.22) followed by enzymatic hydrolysis using an enzymatic cocktail composed of cellulolytic and xylanolytic enzymes. Almost 70% cellulose saccharification was achieved. The remaining cellolignin residue (CLEZ) was analysed for its chemical composition and structural features by conventional wet chemistry methods and a series of spectroscopic tools (FTIR-ATR, solid-state CP/MAS ^{13}C NMR spectroscopy and wide-angle X-ray scattering (WAXS)). The main CLEZ component (about 51%) is acid-insoluble lignin, the chemical composition of which in terms of the ratio of syringyl (S), guaiacyl (G) and *p*-hydroxyphenyl (H) units (70:28:2) is very close to that in the initial bark. This lignin is highly condensed and structurally associated with condensed tannins, which makes CLEZ recalcitrant to delignification by common methods. About one third of cellulose in eucalyptus bark after SE was inaccessible to enzymatic hydrolysis and remained in the CLEZ. This cellulose, structurally similar to microcrystalline cellulose, is imbedded into the lignin-tannins condensed matrix and extremely difficult to purify. In contrast to cellulose, bark hemicelluloses were effectively removed in enzymatic hydrolysis, with only small amounts (<2%) remaining in CLEZ. Among other CLEZ ingredients, proteins and inorganic/organic salts were the most abundant. The latter includes noticeable amounts of calcium oxalate phytoliths (up to 9%), Fe and Si salts. The eventual application areas of CLEZ are discussed.

1. Introduction

The continued depletion of limited fossil resources and their adverse effects on the environment highlights the need to reduce dependence on them. Furthermore, due to the continuous growth of world population and, consequently, increasing energy demand as well as threat of global warming, the biorefinery and circular economy concepts have become imperative in the industrial sector. In the last years, sustainable energy has been on the rise by taking advantage of local agro-industrial residues, such as forestry and agricultural wastes, and by-products of the wood processing industries providing reliable, environmentally friendly, and cost-efficient energy compared with the fossil-based counterpart (Ibitoye et al., 2021; Lisbona et al., 2023). Yet, with the goal of reducing waste-streams and promoting by-products re-circulation into the value chain, the valorisation of the wood processing industries and agro- and forestry residues towards applications for energy and materials production has become an urgent research topic.

Nowadays, *Eucalyptus globulus* is the major source of plantation wood to produce hardwood bleached kraft pulp in South Europe, South America and Africa, due to contributing factors such as fast-growing, easy adaptability to different types of soil and climate conditions, and the high-quality of the ensuing pulp and paper products (Neiva et al., 2015). In Portugal, the consumption of eucalypt wood for pulp production has been increasing in the last years, with an increment of 3.8% in 2021 compared with 2020, which is equivalent to 8.068 Mm^3 of wood free of bark (Biond, 2021). Considering that *Eucalyptus globulus* comprises a bark average volume of 13–18% of the total trunk volume (Miranda et al., 2012, 2015), the amount of bark generated from the pulp and paper industry is such that its valorisation is of great interest. Currently, wood bark is mainly burned for energy production in pulp

* Corresponding author.
E-mail address: dmitrye@ua.pt (D.V. Evtuguin).

https://doi.org/10.1016/j.indcrop.2024.118217
Received 20 November 2023; Received in revised form 11 January 2024; Accepted 5 February 2024
Available online 12 February 2024

mills, or as compost for horticulture uses (Feng et al., 2013). Still, new valorisation routes for bark have been investigated based on its chemical composition and more profitable applications. For instance, some studies have focused on the valorisation of eucalypt bark through liquefaction to produce polyurethane foams (Vale et al., 2019). Eucalypt bark is mostly composed of polysaccharides (ca. 60–65% of cellulose and hemicelluloses), lignin (ca. 16–20%), extractives (ca. 8–12%), hydrolysable and condensed tannins (ca. 10–15%) and ash (ca. 10–15%) (Fernandes et al., 2022; Neiva et al., 2018). In general, eucalypt bark composition approaches that of wood although comprising much higher amounts of extractives, tannins and ash, but lower content of polysaccharides and lignin (Miranda et al., 2012; Miranda and Quilhó, 2018; Neiva et al., 2018). Eucalypt bark is particularly rich in polyphenolic compounds, flavonoids and tannins (Kim et al., 2001; Lima et al, 2018; Santos et al., 2012), which exhibit interesting antioxidant properties. However, the inter-penetrable component matrices and their complex chemical structure in the bark explains its recalcitrance to conversion compared with other non-woody biomasses (Zhu and Pan, 2010). Therefore, biomass pretreatment is required to breakdown the bark structure and mitigate its intrinsic recalcitrance making easier the release of compounds such as fermentable monosaccharides for biofuels (Jacquet et al., 2015).

Among the different biomass pretreatment processes to improve its accessibility to enzymatic hydrolysis, steam explosion (SE) draws special attention (Chen et al., 2017; Zhang et al., 2023a). In particular, SE has been proved to be an efficient, environmental-friendly and industrially scalable process for the deconstruction of lignocellulosic biomass followed by its conversion by enzymatic hydrolysis to fermentable sugars for ethanol production (Fernandes et al., 2015; Foody, 1984; Gao et al., 2021; Mason, 1926; Sarker et al., 2021; Wang et al., 2021; Wyman, 1994). In SE treatment, biomass is rapidly heated using high-pressure saturated steam, generally in the temperature range between 160 ºC and 260 ºC, for a relatively short period of time, ranging from 5 to 30 min, followed by an abrupt depressurization (Tanahashi, 1990; Sarker et al., 2021). During steam pretreatment, partial depolymerization of hemicelluloses and lignin occurs following homolytic and heterolytic pathways (Jacquet et al., 2015; Nader et al., 2022; Sarker et al., 2021). Then, upon sudden depressurization, a rupture of the fibre's cell wall occurs, leading to extensive disaggregation of its tissues and an enormous increase in accessible surface area. Partial rupture of cellulose fibrils in explosive decompression leads to the breakdown of cellulose chains on their surface, which is important for initiating and completing the fermentative hydrolysis of cellulose (Zhang et al., 2023b). A large part of hemicelluloses is converted into soluble sugars or oligosaccharides and a part of lignin becomes soluble in polar organic solvents (Asada et al., 2018; Chadni et al., 2019). In addition to depolymerization, lignin is susceptible to condensation reactions and, when melted and deposited on the surface of the cellulose fibril, it contributes to the recalcitrance of the final cellolignin residue. Similarly to other biomass sources, eucalypt bark can be SE-processed, and the resulting deconstructed residue subjected to enzymatic hydrolysis (EH) to produce fermentable sugars. In the processing of eucalyptus bark via SE, as well as other sources of plant biomass, hemicelluloses are the most vulnerable counterpart to be degraded and removed. Removal of hemicellulose (mainly xylan) can be promoted by combining SE with alkaline treatments (Nader et al., 2022). The residue after bark processing via combined SE/EH treatments is a cellolignin constituted by partially degraded lignin with embedded cellulose inaccessible to the enzymatic attack. This is a new by-product material that is going to be the bottleneck in the processual chain for the production of biofuels and renewable materials or chemical feedstocks and needs urgent utilization solutions (Chen et al., 2017; Jacquet et al., 2015).

In the present study, we examined for the first time the solid lignocellulosic residue of eucalyptus bark remaining from the SE treatment followed by EH and sugar removal. This allows to outline ways for its further utilization to obtain products with increased added value. The chemical composition and structural features of this new waste material was studied by conventional wet chemistry methods and spectroscopic tools (Fourier transform infrared (FTIR) and solid-state cross-polarization/magic-angle-spinning carbon nuclear magnetic resonance (CP/MAS ^{13}C NMR) spectroscopy and wide-angle X-ray scattering (WAXS)). This allowed to infer some possible routes for this by-product utilization.

2. Materials and methods

2.1. Materials

Eucalyptus globulus bark was supplied by RAIZ – Forest and Paper Research Institute (Eixo, Portugal) and collected from The Navigator Company pulp mill (Cacia, Portugal). The eucalypt bark was homogenized in a defined lot and stored in plastic containers at room temperature. Each lot was chemically characterized to determine the exact polysaccharides' content for further use.

Commercial cellulolytic enzyme cocktail Cellic® CTec3 HS, a highly efficient cellulase and hemicellulase complex, was kindly supplied by Novozymes (Bagsvaerd, Denmark) and used for the enzymatic hydrolysis of the steam exploded eucalypt bark. All solvents and other reagents were of analytical grade and were purchased from either Acros Organics Chem. Comp. (Lisbon, Portugal) or Sigma-Aldrich Chem. Comp. (Madrid, Spain).

2.2. Methods

2.2.1. Cellolignin residue

Eucalyptus globulus bark was submitted to a steam explosion (SE) pretreatment to deconstruct feedstock for the further enzymatic hydrolysis (EH) to release fermentable monosaccharides (Scheme 1). This pretreatment consisted in a non-catalyzed steam explosion step initially developed by the STEX® Company (Aveiro, Portugal) in partnership with the National Laboratory of Energy and Geology (LNEG, Lisbon, Portugal). This SE treatment was carried out in a 320 L pilot reactor coupled to a 4000 L blow tank where pretreated biomass is discharged. After a two-step pretreatment at 205 ºC (17.5 bar) for 10 and 3 min, each stage being followed by sudden depressurization of the reactor causing its discharge (total severity factor log R_0 of 4.22), the remaining solid fraction (ca. 85% of pre-treated biomass) was washed with water at room temperature and then directly used for the enzymatic hydrolysis. Eucalyptus bark hydrolysate was obtained after 48 h enzymatic saccharification at 50 ºC of the pretreated solid residue at an initial 175 $g{\cdot}L^{-1}$ solids concentration (oven-dried, o.d., basis), by applying Cellic® CTec3 HS at an enzymatic load of 3% (w/w o.d. solids). This suspension was incubated in a 600 L stirred tank reactor, and the resulting hydrolysate was centrifuged (12000 ×*g*, 15 min, 4 °C) to remove the unreacted solids. The sugars yield was ca. 69% for glucan and ca. 79% for xylan based on their initial content in bark. The unreacted residue, cellolignin residue (CLEZ), was exhaustively washed with water and dried at 40 ºC in a ventilated oven to ca. 5% humidity.

2.2.2. Chemical analysis

Ash content in CLEZ and CLEZ-derived materials was determined gravimetrically by calcination at 525 ± 25 °C according to Tappi standard T 211 om-12. The content and elemental composition of CLEZ's ashes was determined by ICP-MS using a Thermo X Series analyser (Thermo Scientific, Waltham, MA, USA). Elemental analysis was performed to determine the amount of carbon, hydrogen and nitrogen using a LECO CHNS-932 elemental analyser (LECO Corporation, Madrid, Spain). All calculations were made based on solid matter dry weights.

The extractives in *n*-hexane and in acetone were determined by extraction at room temperature for 24 h using liquid-to-solid ratio 100 under vigorous agitation. The extractives in 2% (w/w) of NaOH aqueous solution were determined after CLEZ treatment for 3 h at room temperature under vigorous agitation (liquid-to-solid ratio 100). The

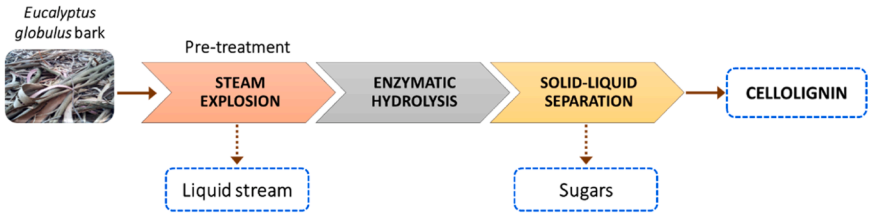

Scheme 1. Flowsheet for the eucalyptus bark processing. Cellolignin (CLEZ) residue was obtained after steam explosion followed by enzymatic hydrolysis.

residue after the alkaline extraction was washed with distilled water and dried to constant weight at 105 ºC. The dissolved matter was calculated as difference between the initial CLEZ weight (oven dried, o.d.) and the sample weight (o.d.) after the extraction. The cellulose was determined according to the Kürschner and Hoffer method, by 4 consecutive treatments of CLEZ with HNO_3:EtOH mixture (1:4, v/v) under reflux for 1 h each (Browning, 1967). The lignin content in CLEZ was determined by Klason method with 72% H_2SO_4 (according to Tappi T 204 om-88). The neutral sugars were analyzed according to previously published procedure, by GC as alditol acetates (Selvendran et al., 1979). The conditions of GC analysis were the same as described previously (Magina et al., 2022).

2.2.3. Image analysis.

Scanning electron microscope (SEM) images of CLEZ grinded powder was acquired using a Hitachi S-4100 microscope and an acceleration voltage of 1.0 kV was applied. (Tokyo, Japan). The powdered sample was placed on the carbon tape surface and the excess was blown. Prior to SEM analysis, the sample was gold-coated.

2.2.4. Protein content

The total protein content was calculated from the elemental analysis (Truong et al., 2013), according to Eq. 1:

$$N \quad content \quad (\%) = (N\% - 0.1) \times 6.25 \tag{1}$$

Where %*N* is the *N* content from elemental analysis and 0.1 is the device error.

2.2.5. FourIer transform infrared spectroscopy (FTIR)

Infrared (FTIR-ATR) spectra of CLEZ, lignin and cellulose products were recorded using a FTIR System Spectrum BX (PerkinElmer, Massachusetts, USA), coupled with a universal attenuated total reflection (ATR) sampling accessory, in absorbance mode from 4000 to 500 cm^{-1} with a 4 cm^{-1} resolution. Samples were analysed as powders, 128 scans were averaged, and all spectra were baseline corrected and normalized (using the min-max normalization technique (Gautam et al., 2015)) for further analysis.

2.2.6. Analytic pyrolysis

Analytical pyrolysis (Py-GC/MS) was performed as follow: wood samples were extracted in Soxhlet apparatus sequentially with dichloromethane, ethanol, and water for 8 h each. CLEZ sample was extracted by *n*-hexane. Then, around 0.10 mg of extractives-free sample was weighted and analysed by analytical pyrolysis apparatus (Py) coupled to a gas chromatograph Agilent 7890B (Santa Clara, USA) and mass detector Agilent 5977B (Santa Clara, USA). The sample was pyrolyzed at 550 °C (for 1 min) in a platinum coil Pyroprobe connected to a CDS 5150 valved interface linked to the GC-MS and having installed a fused-silica capillary column (ZB-1701: 60 m x 0.25 mm i.d. x 0.25 μm film thickness). The chromatographic conditions used were as follows: 40 °C (held for 4 min), then increased to 100 °C at 20 °C·min^{-1}, and then to 270 °C at 6 °C·min^{-1} (held for 5 min). The temperature of the injector was 270 °C, the MS interface was 280 °C, and applied electron ionization energy of 70 eV. Helium was the carrier gas with a total flow of 1 mL·min^{-1}. The compounds were identified comparing their mass spectra with databases (Wiley and NIST2014) and literature (Ralph and Hatfield, 1991). Each identified compound was automatically calculated based on its integrated area and the total area of the chromatogram.

2.2.7. Thermogravimetric analysis (TGA)

TGA of the samples was carried out using a Setsys Evolution 1750 TGA-DSC (Setaram, Caluire, France) thermogravimetric analyser equipped with a DSC plate rod accessory and the thermal analysis software Setsoft 2000. Samples were analysed from room temperature up to 800 °C at a heating rate of 10 °C·min^{-1} under nitrogen flow rate of 200 mL·min^{-1} using an alumina crucible. A blank experiment (with empty crucible) was carried out under the same conditions for each type of experiments prior the experiments with samples, to subtract the buoyancy effect. Temperature and heat flow calibrations were carried out using the melting points of four standards (In, Pb, Al, and Au) at three different heating rates (5, 10, and 15 °C·min^{-1}).

2.2.8. Isolation of dioxane lignin

Lignin was isolated by acidolysis from CLEZ under nitrogen atmosphere by the dioxane method adapted from a previously published procedure (Evtuguin et al., 2001), with some adjustments, as follows: CLEZ (10 g, based on a dry matter) was placed in a 1-L two-necked rounded flask with a reflux condenser and a nitrogen inlet, and then 200 mL of a mixture of dioxane/water (9:1, v/v) containing 0.73 g of hydrogen chloride (equivalent to 0.1 M solution) was added slowly. The reaction mixture, under nitrogen flow, was heated using an electric heating mantle equipped with an adjustable thermal regulator and refluxed for a period of 45 min. Then, the mixture was allowed to cool down to around 50 °C under nitrogen atmosphere. The liquid phase was then decanted, and the solid residue was subjected to the next extraction with 200 mL of fresh acidic dioxane/water solution for 45 min. This extraction procedure was carried out twice more. The last (fourth) extraction was carried out using the mixture of dioxane/water (9:1, v/v) without the addition of hydrochloric acid. Each portion of extract was concentrated separately using a rotary evaporator to reduce a volume from 200 mL to around 40 mL. The obtained concentrates were combined, and the lignin was precipitated by addition of the lignin-containing dioxane solution into cold water (about 1500 mL). The supernatant was removed, and the lignin-precipitated fraction was centrifuged, washed with distilled water and vacuum-oven dried at 35 ºC. The residue from the isolation of dioxane lignin was used for the subsequent analysis of cellulose employing Kürschner and Hoffer method.

2.2.9. Solid state nuclear magnetic resonance (NMR) spectroscopy

Solid-state CP/MAS ^{13}C NMR spectra were recorded using a Bruker Avance III spectrometer (Bruker, Wissembourg, France) operating at 400 MHz and using a 4 mm zirconia rotor sealed with Kel-F™ caps. The rotor's spinning speed was 12 kHz, contact time 1 ms, ca. 7000 scans with a 90° proton pulse were collected with a recovery delay of 2.5 s. About 9000 scans were collected. Glycine was used as an external standard for the calibration of the chemical shift scale relative to tetramethylsilane ($(CH_3)_4Si$), following the Hartman-Hahn matching procedure. The crystallinity index (*CrI*) of cellulose was determined by the C4 peak separation method, i.e., by separating the C4 region of the

cellulose spectrum to crystalline and amorphous peaks, and calculating *CrI* by dividing the area of the crystalline peak (from 86 to 92 ppm, $A_{86–92}$) by the total area assigned to the C4 peak (from 80 to 92 ppm, $A_{80–92}$) (Newman, 2004; Park et al., 2010), according to Eq. 2:

$$CrI, \% = \frac{A_{86-92ppm}}{A_{86-92ppm} + A_{80-86ppm}} \quad (2)$$

2.2.10. X-ray scattering analysis

Isolated cellulose samples were analysed by wide-angle X-ray diffraction scattering (WAXS) as textured samples (pellet of ca. 1 mm thickness and around 1.2 cm diameter of cellulose was pressed at 50 MPa) by in a Philipps X'Pert MPD diffractometer using Cu-Kα source (λ = 0.154 nm) in the 2θ range 2–40° and scanning step width of 0.02 °/scan. The crystallinity index (*CrI*) of cellulose was determined according to the Segal peak height method (Ahvenainen et al., 2016; Segal et al., 1959), given by Eq. 3:

$$CrI = \frac{I_{200} - I_{am}}{I_{200}} \quad (3)$$

where I_{200} is the intensity value of the 200 reflection peak and I_{am} is the intensity value at 2θ = 19° respective to the maximum of amorphous halo.

The average width of crystallite was determined in the 200-lattice plane (D_{200}) using the Scherer equation (Eq. 4):

$$D_{200} = \frac{K \cdot \lambda}{\beta \cdot \cos\theta} \quad (4)$$

where K is the shape factor (0.89 for cellulose), λ is the X-ray wavelength (0.154 nm), θ is the diffraction angle at the maximum of 200 reflex and β is the width at half-peak-height of the 200 reflex (rad).

3. Results and discussion

3.1. Chemical composition of cellolignin residue

The results on the cellulose conversion upon saccharification of steam-exploded eucalyptus bark were quite comparable to those previously reported for hardwoods and shrubs while employing similar severity of SE treatment and comparable conditions of enzymatic hydrolysis by industrial cellulases (Table 1). This is due to a certain similarity of these plant materials in terms of cellular morphology and the chemical composition. In this sense, grasses having less recalcitrant morphology and containing more easily removable lignin in the SE treatment (Gao et al., 2021; Montipo et al., 2020) commonly demonstrate easier processability with greater yield of cellulose-derived sugars (Table 1).

Table 1
Results of cellulose saccharification after steam explosion/enzymatic hydrolysis processing of plant biomass.

Plant material	log R_0*	Enzymatic hydrolysis* *	Converted cellulose (%)	Reference
Aspen wood	4.25	24 h; 55 °C; pH 4.6	71	Horn and Eijsink (2010)
Mixed hardwoods	4.25	24 h; 55 °C; pH4.6	67	Horn and Eijsink (2010)
Eucalyptus bark	4.22	48 h; 50 °C; pH 5.0	69	This study
Cardoon	3.97	72 h; 50 °C; pH 4.8	68	Fernandes et al. (2015)
Eel grass	3.06	72 h; 50 °C; pH 5.0	90	Viola et al. (2008)
Elephant grass	3.20	72 h; 50 °C; pH 4.8	85	Montipo et al. (2020)

* Severity factor $R_0 = t \times e^{\frac{(T-100)}{14.75}}$, where t is a treatment duration (min) and T is a treatment temperature (°C). * *Conditions of enzymatic hydrolysis using industrial cellulases.

The cellolignin residue (CLEZ) remaining after enzymatic hydrolysis of eucalyptus bark processed by steam explosion represents a dark powder, which looks like disrupted bark particles of various sizes and shapes (Fig. 1). This feature is expectable due to the harsh conditions of steam explosion process and is due to physical rupture of bark structure via adiabatic expansion of water within bark tissues with autohydrolysis of cell wall components (Tanahashi, 1990). The general chemical composition of CLEZ was primary assessed using conventional wet chemistry methods (Table 2). The lignin and cellulose appeared to be the main constituents of CLEZ contributing ca. 51% and 17%, respectively. Hence, the amount of lignin almost triplicate in CLEZ when compared with that in the bark, which is commonly about 16–17% (Fernandes et al., 2022). In opposite, the amount of cellulose in CLEZ was less than half to that in the bark (40–41%). The content of hemicelluloses in CLEZ was very low (Table 2), although their content in the initial bark (ca. 23%) is quite significant (Fernandes et al., 2022). These facts are consistent with general purposes of the bark saccharification, which presumes its structural disintegration by SE pre-treatment and extensive hydrolysis of polysaccharides by enzymatic cocktail (mixture of cellulase and xylanase). Some higher lignin content detected in CLEZ that could be predicted by removal of hemicelluloses and cellulose from bark can be assigned to concomitant tannins present in bark, which contributed to the analysis of Klason lignin (Fernandes et al., 2022).

The ash content in CLEZ (Table 2) was comparable to the values normally reported in eucalyptus bark (Fernandes et al., 2022; Neiva et al., 2018) meaning that at least part of the inorganics were soluble in water and removed during SE and enzymatic hydrolysis hydrolysis operations. The ash composition revealed the major contribution of Ca, Fe and Na salts followed by salts of K, Al, Mn and Mg (Table S1, Supplementary data). Additionally, a noticeable amount of silica was also detected. A major part of Ca might associated with the composition of the calcium oxalate phytoliths (Quilhó et al., 1999) and the relatively high amounts of Fe salts is a peculiarity of the chemical composition of the *E. globulus* bark (Neiva et al., 2018).

The presence of proteins (about 5%) was suggested based on the notable nitrogen content in CLEZ. Proteins are present in the initial bark before treatment and may result from the glycoprotein counterpart of cellulolytic enzymes eventually adsorbed on CLEZ (Horn and Eijsink, 2010). In fact, the relatively high protein content in the bark of fast-growing eucalyptus species is explained by its important role in the primary metabolism of the phloem (Budzinski et al., 2016).

The extractives of CLEZ were analysed using non-polar (*n*-hexane) and polar (acetone) solvents to assess aliphatic non-oxygenated and

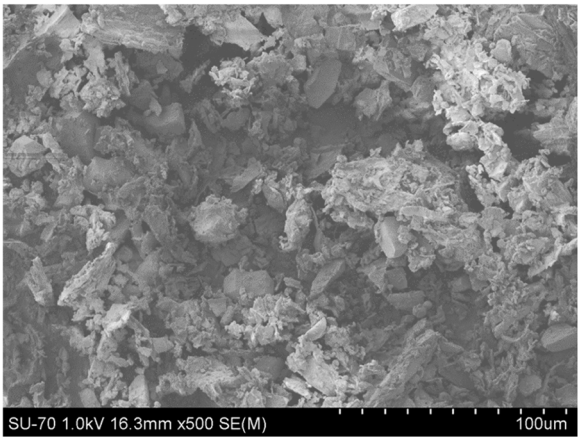

Fig. 1. SEM image of CLEZ residue. Cellolignin particles containing inaccessible highly crystalline cellulose embedded in the lignin matrix.

Table 2
Chemical composition of CLEZ.

Chemical components (% wt.)		Content
Ash		12.8 ± 0.2
Extractives		
	In *n*-hexane	0.66 ± 0.00
	In acetone	11.7 ± 0.4
Insoluble lignin (Klason)* *		50.8 ± 0.4
Elementar analysis		
	C	46.5 ± 0,1
	H	5.1 ± 0.4
	N	0.96 ± 0.04
Proteins*		5.3 ± 0.2
Cellulose (Kürschner-Hoffer)		17.0 ± 0.5
Polysaccharide analysis		15.2 ± 1.9
	Rhamnan	0.08 ± 0.02
	Arabinan	0.05 ± 0.01
	Xylan	0.64 ± 0.03
	Mannan	0.32 ± 0.03
	Galactan	0.08 ± 0.01
	Glucan	14.0 ± 1.9

* calculated based on the nitrogen content. * *corrected for the ash and protein contaminants.

oxygenated extractive compounds, respectively. The amount of extractives soluble in hexane was moderate (about 0.7%) and similar to that reported previously for extractives in non-polar solvents in eucalyptus bark (Fernandes et al., 2022; Neiva et al., 2018). According to preliminary analysis, the main constituents of these extractives were fatty acids and sterols and their derivatives (data not presented). In contrast to hexane extractives, the extractives in acetone were quite abundant, almost 12%, and looked as a dark highly viscous product, not typical for bark extractives. According to data on acetone extracts from different sources of plant biomass processed by SE, they are normally largely composed of low molecular weight lignin degradation products (Asada et al., 2018; Hemmingson, 1987). These lignin degradation products can have some practical value in the synthesis of lignin-based adhesives (Asada et al., 2018). Among the identified acetone extractives components, the most abundant were sugars derivatives and small amounts of monomeric phenolics such as vanillin and syringaldehyde (data not presented). The relatively low percentage of the identified products by GC-MS analysis (less than 20%) may be explained by relatively high proportion of non-volatile oligomeric lignin degradation products.

The significant amount of lignin and cellulose in CLEZ was confirmed by FTIR spectroscopy (Fig. 2). Indeed, FTIR-ATR spectrum of CLEZ exhibits characteristic bands of both lignin and polysaccharides confirming that removal of cellulose was incomplete. The strong band between 3030 and 3680 cm^{-1} is assigned to stretching of hydroxyl groups present mainly in polysaccharides and, in smaller extent, in lignin (Agarwal and Atalla, 2010; Carrillo et al., 2018). The bands at 2918 and 2840 cm^{-1} are assigned to the stretching vibration of C–H of aliphatic methylene/methyl and methoxy groups, respectively. The characteristic lignin bands were found at 1596, 1504 and 1425 cm^{-1} assigned to aromatic skeletal vibrations in S/G type of lignin, and the relatively intensive band at 1452 cm^{-1} related also to the C–H bond vibration in the methoxyl group in lignin (Boeriu et al., 2004; Hergert, 1971). The strong intensity bands at 1108 and 1030 cm^{-1} are characteristic of C–OC and C–OH deformations, respectively, in lignin and polysaccharides (Fig. 2). The prevalence of the band at 1030 cm^{-1} and strong intensity band at ca. 3400 cm^{-1} may be indicative for the presence of significant amount of polysaccharides. This fact was additionally confirmed by the solid-state ^{13}C NMR results of CLEZ (Fig. 3), which revealed characteristic resonances from cellulose (Table 3). Thus, strong resonances from carbons involved in glycosidic bonds (semiacetal C1 at 104.8 ppm and C4 in crystalline and amorphous cellulose at 80–90 ppm) and carbons linked to secondary alcohol groups (C2, C3), in the pyranose ring (C5) and to primary hydroxyls (C6) were clearly identified (Fig. 3, Table 3).

The lignin aromatic carbon resonances of CLEZ were registered in the solid-state ^{13}C NMR spectrum range of 102–162 ppm (Fig. 3). The relatively intensive resonance at 55.4 ppm, assigned to carbon atom in methoxyl groups, indicated the eventual strong contribution of syringyl structural units. This is confirmed by the strong resonance centred at 152.5 ppm, assigned to the C3 and C5 atoms in syringyl lignin units (Table 3), which was, however, inferior to the resonance peak centred at 147.2 ppm, assigned to C3 in guaiacyl units (Fig. 3). However, this group of quaternary oxygenated aromatic carbons at 143–148 ppm also includes the C4 resonances of phenolic syringyl lignin units and tannins (Table 3). Therefore, the lower intensity signal at 152.5 ppm that at 147.2 ppm does not mean at all the prevalence of guaiacyl over syringyl units in CLEZ but instead indicates the strong depolymerization of lignin fragments constituted by syringyl units. The strong resonances at 130–138 ppm are commonly assigned to C1 in lignin structural units and to other quaternary aromatic carbons belonging to condensed structures and tannins. The extensive lignin condensation during SE processing of biomass has been extensively discussed (Fernandes et al., 2015; Li et al., 2020; Obame et al., 2019; Tanahashi, 1990). The thermochemical treatment can also result in lignin condensation with tannins, especially under acidic conditions (Ping et al., 2011; Prozil et al., 2014). The strong multiple resonances at 166–169 ppm (Fig. 3) were assigned to the oxalic acid in CLEZ composition (Trouvé et al., 2023). In fact, the significant amounts of poorly soluble calcium oxalates present in the bark from eucalyptus species (Quilhó et al., 1999) and their appearance in the bark residue after SE and enzymatic hydrolysis is not surprising. If assuming all calcium salts as calcium oxalates and considering the Ca content in CLEZ (Table S1, Supplementary data), the total calcium oxalate content in CLEZ can be estimated at ca. 9% (w/w).

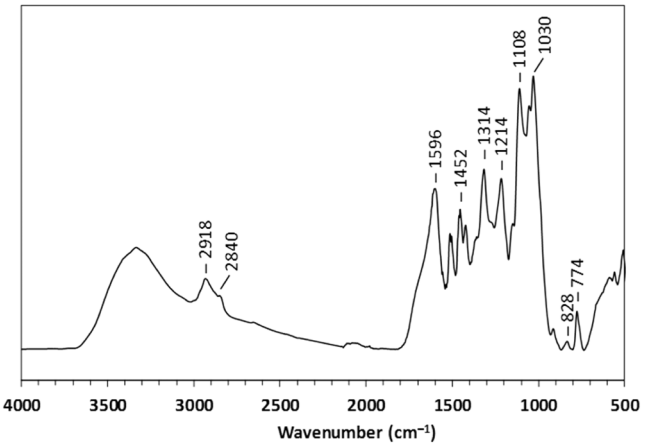

Fig. 2. FTIR-ATR spectrum of the cellulolignin solid residue, CLEZ.

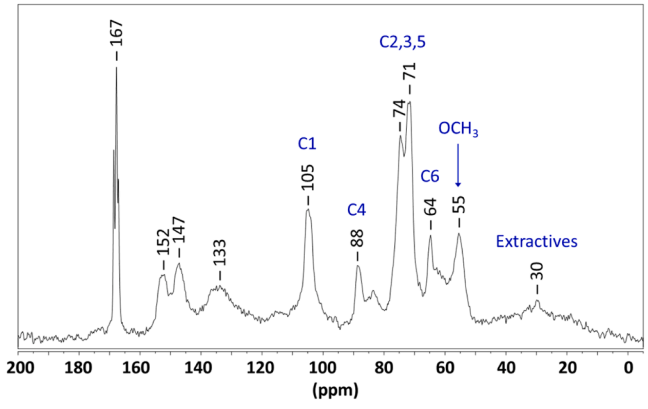

Fig. 3. Solid-state ^{13}C CP-MAS NMR spectrum of CLEZ. The assigned carbon atoms C1-C6 are from cellulose and methoxyl carbon from lignin.

Table 3
Assignments of carbon signals in solid-state CP-MAS ^{13}C NMR spectrum of CLEZ (Gao et al., 2015; Gilardi et al., 1995; Hawkes et al., 1993; Rachocki et al., 2008).

Chemical shift (ppm)	Assignment
15 – 35	Extractives
52 – 60	OCH_3 groups in lignin
63 – 66	C6 in cellulose, C5 in hemicellulose (xylan)
70 – 85	β-O-4′ in G and S units (Cα and Cβ) in lignin
70 – 80	C2, C3 e C5 in cellulose and hemicelluloses;
80 – 90	C4 in cellulose/hemicellulose; Cβ in β-O-4 lignin structures
102 – 110	C2 and C6 in S units
105	C1 in cellulose
110 – 125	C2, C5 and C6 in G units
125 – 137	Quaternary C in condensed lignin
133-138	C1 in G and S lignin units
145 – 148	C3 and C4 in phenolic/non-phenolic G and S units
152 – 153	C3 and C5 in non-phenolic S units
166-170	Carbons in oxalic acid

Such significant amounts of oxalic acid may be interesting from the point of view of its practical use.

The referred peculiarities in chemical composition of CLEZ facilitates the better understanding of the thermal behaviour of this residue under nitrogen atmosphere (Fig. 4). Considering that the weight loss of sample at 50–100 ºC is due to adsorbed water, the maximum weight loss at ca. 145 and 186ºC can be assigned to the loss of water molecules in crystal hydrates of different organic/inorganic salts. Thus, calcium oxalate monohydrate looses water at exactly 145–150 ºC (Trouvé et al., 2023). The main weight loss (ca. 40%) occurs in the temperature range of 300–400 ºC with maximum rate at 358 ºC assigned to thermal decomposition of lignin and cellulose with release of volatile degradation products. The second maximum at about 500 ºC corresponds to the structural arrangements associated with char formation (charring) (Brebu and Vasile, 2010). The maximum weight loss at 629 ºC is attributed to structural changes in the char that lead to its structural densification. Noteworthy is the fact that in the same temperature range the thermal degradation of inorganic salts also takes place. For example, the thermal degradation of calcium oxalate led to calcium carbonate formation, which is in turn decarbonized into lime between 600 and 700 ºC (Trouvé et al., 2023).

3.2. Structural features of lignin in CLEZ

Attempts to isolate representative lignin from CLEZ by acetone extraction with the yield of 11.7% (Table 2) or by common acidolytic technique using dioxane:water solution (9:1, v/v, 0.2 M HCl) with the yield of 15.3% (wt.) can only be considered partially successful. The extraction with 2% NaOH solution afforded a better result (yield of ca. 22%), but with strong contamination with ash. Such unusual recalcitrance of lignin counterpart in CLEZ apparently comes from its inaccessibility related also with structural association with other degraded bark counterparts. This is in agreement with a previous work that reported the significant deterioration of soda cooking of SE processed eucalyptus bark (Nader et al., 2022).

The FTIR-ATR spectra of acetone extract (AEX) and dioxane lignin (DLEZ) were similar and showed characteristic bands as discussed previously for parent CLEZ (Fig. 5). However, AEX and DLEZ contained relatively sharp bands centred at ca. 1690–1700 cm^{-1}, which can be assigned to conjugated carbonyl groups. This band is commonly reported for degraded lignins obtained in acidolytic procedures being assigned to Hibbert ketones (Evtuguin et al., 2001). Hibbert ketones arise in SE treatment of biomass and their detection serves as evidence of acidolytic mechanisms involved in lignin degradation (Obame et al., 2019). Both AEX and DLEZ revealed the bands at 1322 and 1214 cm^{-1} assigned to syringyl and guaiacyl ring breathing vibrations, respectively, thus clearly confirming the S/G type of isolated lignins (Agarwal and Atalla, 2010; Hergert, 1971). The lower intensity of bands at ca 3360 cm^{-1} (O-H stretching in hydroxyls) and 1022 cm^{-1} (C-OH stretching in alcohols) in AEX than in DLEZ indicates less contamination with carbohydrates of the former. This is understandable taking into consideration the purification step involved in DLEZ isolation.

The basic composition and structural features of lignin in CLEZ were assessed using isolated acid insoluble lignin (Klason lignin). Although Klason lignin does not reflect the exact structure of the lignin in CLEZ, it still reflects its main structural composition and the presence of non-lignin concomitants. This lignin contained a small proportion of extractives in hexane (ca. 0.7%), ash (ca. 0.8%) and proteins (ca. 3.8%) (Table 4). The structural analysis of Klason lignin from CLEZ was carried out by solid-state ^{13}C NMR spectroscopy (Fig. 6), which showed typical lignin resonances (Table 3) and the absence of signals from polysaccharides (cellulose and xylan) and oxalates, as opposed to the spectrum of CLEZ (Fig. 3), thus confirming the entirety of polysaccharide hydrolysis and removal of oxalate phytoliths upon determination of the acid insoluble lignin. Particular attention should be given to the unusual strong group of resonances at 10–40, 120–130 and 140–145 ppm (Fig. 6). The intensity of these resonances is commonly quite low in lignin and indicates possible lignin concomitants. Strong resonances at 10–40 ppm cannot be assigned exclusively to extractives with aliphatic chains, because the determined amount of extractives in Klason lignin was relatively low (Table 4). Previously, the unusually strong resonances centred at ca. 30 ppm in Klason lignin from grape stalks were assigned to methylene moieties in catechin and gallocatechin structural units of condensed tannins structurally associated to lignin (Prozil et al., 2012). The resonances at 120–130 and 140–145 ppm are other characteristic resonance groups from condensed tannins assigned to respective aromatic tertiary and quaternary oxygenated carbons. The strong condensation of isolated Klason lignin is also evidenced from strong resonances at 130–140 ppm (Fig. 6) assigned to quaternary

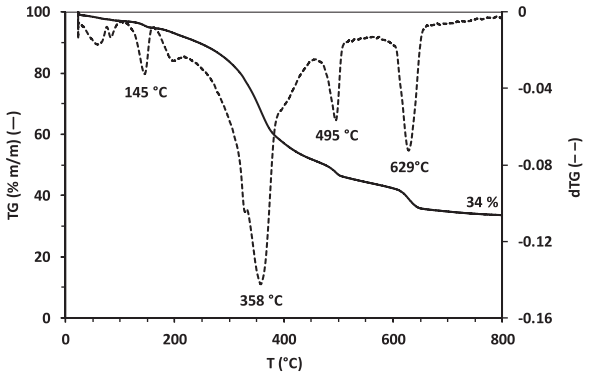

Fig. 4. TGA and DTG curves of CLEZ under inert atmosphere (N_2).

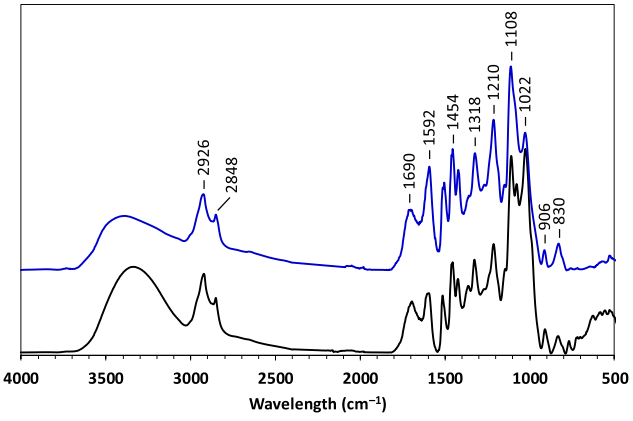

Fig. 5. FTIR-ATR spectra of acetone extract (AEX, lower spectrum), and dioxane lignin (DLEZ, upper spectrum) isolated from CLEZ.

Table 4
Chemical analysis of Klason lignin isolated from CLEZ.

Chemical composition (%, wt.)	Content
Klason lignin	56.0 ± 0.4
Ash	0.80 ± 0.02
Extractives (*n*-hexane)	0.66 ± 0.00
Proteins*	3.77 ± 0.05
Klason lignin – corrected value	50.8 ± 0.4

* calculated based on the nitrogen content in the sample.

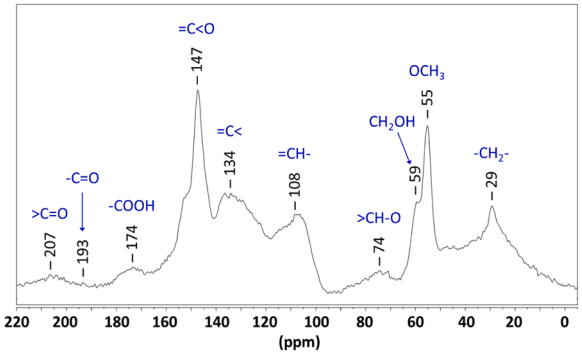

Fig. 6. CP-MAS ^{13}C NMR spectrum of Klason lignin from CLEZ.

non-oxygenated aromatic carbons (Table 3). However, this condensation could occur both during SE and during the determination of acid-insoluble (Klason) lignin.

The eventual structural association of lignin in CLEZ with condensed tannins can explain the detected recalcitrance of lignin isolation from CLEZ. Previously, similar features were reported for the lignin in grape stalks material, which showed extremely high resistance to delignification either under acid-catalysed organosolv (Ping et al., 2011) or kraft delignification (Prozil et al., 2012) due to the strong condensation with concomitant condensed tannins. Hence, isolation of lignin from SLEZ requires advanced approaches capable of effectively degrading the condensed lignin network (e.g., appropriate oxidative methods).

The structural composition of lignin in CLEZ was assessed using analytic pyrolysis (Py-GC/MS). The detailed results on the identification of CLEZ pyrolysis products are presented in Table S2 (Supplementary data). The summarized data (Table 5) indicate that the molar ratio between the S, G and H lignin structural units was 70:28:2, just very close to the same proportions previously reported for eucalyptus bark (72:26:2) by Gominho et al. (2021). Special attention should be given to the detection of volatile pyrolysis products such as catechol and orcinol, which are almost absent in the (Py-GC/MS) analysis of different eucalyptus species (Table S2, Supplementary data). These pyrolysis products are normally assigned to condensed tannins in biomass sources (Galletti and Reeves, 1992) thus confirming their significant contribution to CLEZ.

Table 5
Quantification of the pyrolysis analysis from eucalypts bark (extractives-free) and CLEZ.

Detected products	Eucalyptus bark*	CLEZ
Total carbohydrate degradation products (%)	46.5	27.3
Total lignin degradation products (%)	27.4	55.1
Other lignin derivatives (%)	-	2.3
S:G:H ratio	72:26:2	70:28:2

* As reported by Gominho et al. (2021). S, G and H designate syringyl, guaiacyl and *p*-hydroxyphenyl units, respectively.

3.3. Structural features of cellulose in CLEZ

The cellulose in CLEZ was isolated by the Kürschner-Hoffer method from the residue obtained after the isolation of the dioxane lignin. The yield was of 17.0% based on the weight of initial CLEZ involved in the analysis. However, the isolated cellulose still had some brownish colour (Fig. 7a) most likely due to the presence of chromophores from residual lignin and degraded tannins. Therefore, this cellulose was submitted to a bleaching process with peracetic acid (90 °C; 10 min) resulting into a brighter material (Fig. 7b) with 16.4% yield (based on the CLEZ). This cellulose residue was composed almost completely by glucan with only small contamination of polyoses based on the sugars analysis. Thus, CLEZ cellulose isolation is associated with the need for several purification steps with the aim of completely removing residual lignin. This bleached cellulose was used for further analysis.

The analysis of cellulose isolated from CLEZ by solid-state ^{13}C NMR revealed typical spectral patterns of cellulose I polymorph containing both cellulose I_α and I_β phases (Fig. 8). Thus, clearly distinguishable signals at 104 and 105 ppm are assigned to anomeric carbon (C1) in monoclinic (I_β) and triclinic (I_α) cell units (Atalla and Vanderhart, 1999). The ratio of signals centred at 88.6 ppm and at 84.0 ppm arisen mainly from ordered and disordered cellulose regions, respectively (Atalla and Vanderhart, 1999; Liitiä et al., 2000), clearly indicative of the significant content of crystalline phase of cellulose. The estimated *CrI* of 58% was similar to that detected by the same methodology (57%) previously by Park and co-workers (Park et al., 2010) for the microcrystalline cellulose (MCC).

More detailed structural information was obtained from cellulose analysis by WAXS (Fig. 9). The X-ray diffractogram shows the typical profile of cellulose I including the characteristic peaks with the maxima at about 14.8°/16.2°, 22.7° and 34.6°corresponding to 1–10/110, 200 and 040 planes, respectively. The crystallinity index calculated from WAXS diffractogram by Segal method was 87%, very close to the respective value of 92% reported for the MCC (Park et al., 2010). The average crystallite width (D_{200}) of cellulose obtained from CLEZ was 4.0 nm. This value is lower than the D_{200} reported for cellulose from *E. globulus* wood (5.0–5.6 nm) (Lourenço et al., 2020; Rebuzzi and Evtuguin, 2005). This fact can be explained, at least partially, by changes occurred during SE and enzymatic hydrolysis. Thus, thermal treatment at temperatures higher than 200 °C can lead to some amorphization of fibril surfaces (Lourenço et al., 2020), which are further readily attacked by cellulolytic enzymes that peels off the fibrils. This fact of decreasing crystallite width may be important for applications where this factor is important.

4. Conclusions

The most abundant component of the cellolignin residue (CLEZ) remaining after steam explosion (SE) followed by enzymatic hydrolysis of *Eucalyptus globulus* bark was found to be highly condensed acid-insoluble lignin (ca. 51% w/w) structurally associated with condensed tannins. This is the main factor of recalcitrance in lignin isolation from CLEZ. The molar ratio of S:G:H structural units in CLEZ lignin (70:28:2) was close to that typically reported for bark lignin. The partially degraded lignin in CLEZ reveals a greater amount of phenolic and ketone structures, providing it with additional chelation capacity and potential in modification reactions. A significant part of bark cellulose (almost one third), embedded into highly condensed lignin matrix after SE, was inaccessible to enzymatic hydrolysis and remained in CLEZ. This cellulose possesses relatively high crystallinity similar to that reported for microcrystalline cellulose (MCC). The crystallite cross dimension of the residual cellulose in CLEZ was almost 20% inferior to that in wood. A relatively high content of ash is a distinctive feature of CLEZ, the major contribution being from Ca and Fe salts and silicates. The particularly high abundance of Ca was attributed to the high content of poorly soluble calcium oxalate phytoliths in the bark (up to 9%). The relatively

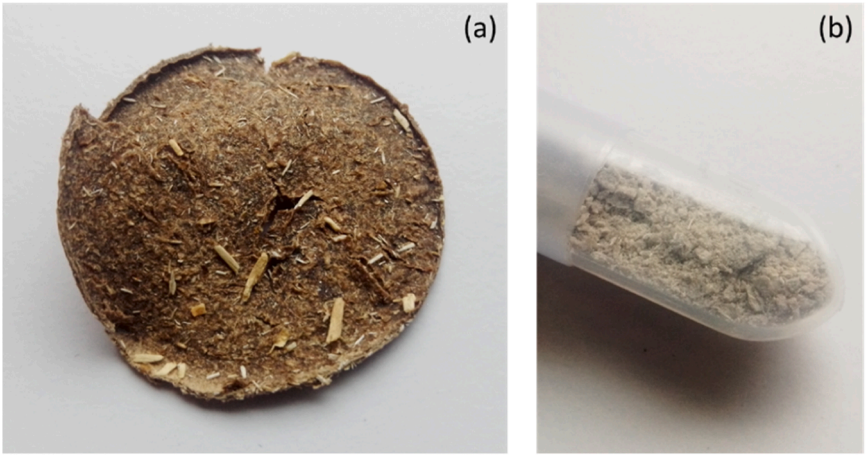

Fig. 7. Cellulose isolated using the Kürschner-Hoffer method (a), and cellulose after bleaching/delignification with peracetic acid (b).

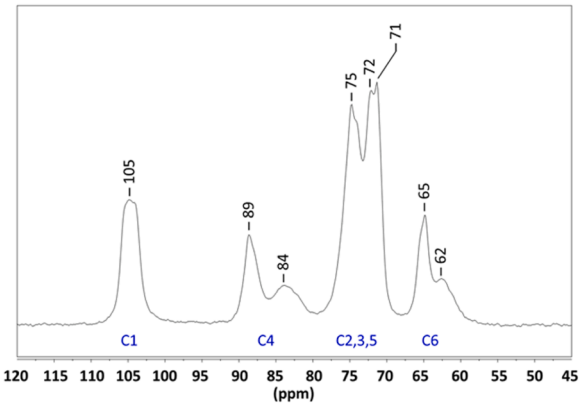

Fig. 8. Solid-state CP-MAS ^{13}C NMR spectrum of cellulose from CLEZ with assigned carbon atoms.

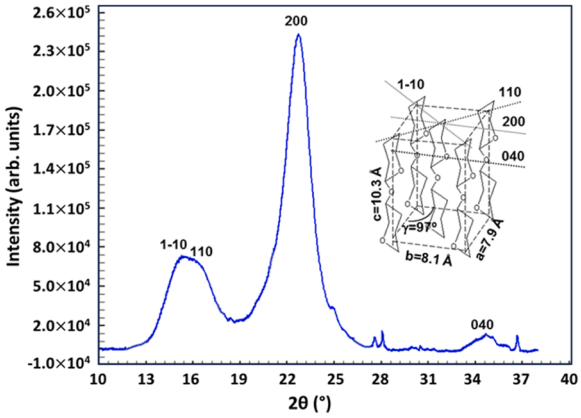

Fig. 9. WAXS diffractogram of cellulose from CLEZ. The basic elementary cell unit dimensions and lattice plans are shown in the upper right corner.

high content of proteins (up to 5%) is another peculiar feature of CLEZ. The relatively low content of polyoses in CLEZ (1–2%) proves the effectiveness of their conversion by SE processing combined with enzymatic hydrolysis. Knowledge of the chemical composition and general structural characteristics of CLEZ components provides the fundamental basis for the search for new ways of using this by-product that can be inferred but are not limited to bioremediation and biocomposite materials, adhesives, nanostructured composites and biochemicals. Crucial advances are expected in effectively fractionating CLEZ into lignin and cellulose counterparts, studies of which are ongoing.

CRediT authorship contribution statement

Gírio Francisco: Writing – review & editing, Validation, Resources, Methodology. **Magina Sandra:** Writing – original draft, Methodology, Investigation, Formal analysis, Conceptualization. **Marques Susana:** Writing – review & editing, Validation, Resources, Methodology. **Evtuguin Dmitry V.:** Writing – review & editing, Validation, Supervision, Methodology, Funding acquisition, Conceptualization. **Lourenço Ana:** Writing – review & editing, Visualization, Investigation, Formal analysis. **Barros-Timmons Ana:** Writing – review & editing, Validation, Supervision, Project administration.

Declaration of Competing Interest

The authors declare that they have no known competing financial interests or personal relationships that could have appeared to influence the work reported in this paper.

Data Availability

Data will be made available on request.

Acknowledgements

This work was developed within the scope of the project CICECO-Aveiro Institute of Materials, UIDB/50011/2020 (DOI 10.54499/UIDB/50011/2020), UIDP/50011/2020 (DOI 10.54499/UIDP/50011/2020) & LA/P/0006/2020 (DOI 10.54499/LA/P/0006/2020) and CEF, http://doi.org./10.54499/UIDB/00239/2020, both Centres financed by national funds through the FCT/MCTES (PIDDAC). The authors acknowledge the financial support from Integrated Project BE@t – Textile Bioeconomy, to strengthen the National Bioeconomy, financed by the Environmental Fund through Component 12 – Promotion of Sustainable Bioeconomy (Investment TC-C12-i01 – Sustainable Bioeconomy No. 02/C12-i01/202), of European funds allocated to Portugal by the Recovery and Resilience Plan (RRP), within the scope of the European Union (EU) Recovery and Resilience Mechanism, framed in the Next Generation EU, for the period 2021 – 2026. The authors gratefully acknowledge RAIZ – Forest and Paper Research Institute (Eixo, Portugal) for providing the *Eucalyptus globulus* bark collected from the Navigator company pulp mill (Cacia, Portugal), and Novozymes (Bagsvaerd, Denmark) for supplying Cellic® CTec3 HS. The technical assistance of STEX Company (Aveiro,

Portugal) on the operation of pilot scale infrastructure of steam explosion and enzymatic hydrolysis is also acknowledged. The NMR spectrometers are part of the National NMR Network (PTNMR) and partially supported by Infrastructure Project Nº 022161 (co-financed by FEDER through COMPETE 2020, POCI and PORL and FCT through PIDDAC). A. L. was also supported by FCT through a research contract (http://doi.org/10.54499/DL57/2016/CP1382/CT0007).

Appendix A. Supporting information

Supplementary data associated with this article can be found in the online version at doi:10.1016/j.indcrop.2024.118217.

References

Agarwal, U.P., Atalla, R.H., 2010. Vibrational spectroscopy. In: Heitner, C., Dimmel, D., Schmidt, J.A. (Eds.), Lignin and Lignans: Advances in Chemistry. Taylor and Francis Group. LLC, Boca Raton, FL, pp. 103–136.

Ahvenainen, P., Kontro, I., Svedström, K., 2016. Comparison of sample crystallinity determination methods by X-ray diffraction for challenging cellulose I materials. Cellulose 23, 1073–1086. https://doi.org/10.1007/s10570-016-0881-6.

Asada, C., Sasaki, C., Suzuki, A., Nakamura, Y., 2018. Total biorefinery process of lignocellulosic waste using steam explosion followed by water and acetone extractions. Waste Biomass-.-. Valoriz. 9, 2423–2432. https://doi.org/10.1007/s12649-017-0157-x.

Atalla, R.H., Vanderhart, D.L., 1999. The role of solid state 13C NMR spectroscopy in studies of the nature of native celluloses. Solide State Nucl. Magn. Reson. 15, 1–19. https://doi.org/10.1016/S0926-2040(99)00042-9.

Biond, 2021. Statistics Bulletin 2021 - Forest fibers from Portugal.

Boeriu, C.G., Bravo, D., Gosselink, R.J.A., van Dam, J.E.G., 2004. Characterisation of structure-dependent functional properties of lignin with infrared spectroscopy. Ind. Crops Prod. 20, 205–218. https://doi.org/10.1016/j.indcrop.2004.04.022.

Brebu, M., Vasile, C., 2010. Thermal degradation of lignin - a review. Cellul. Chem. Technol. 44, 353–363.

Browning, B.L., 1967. Methods of wood chemistry, Vol. 2. Interscience Publishers Inc, New York.

Budzinski, I.G.F., Moon, D.H., Morosini, J.S., Lindén, P., Bragatto, J., Moritz, T., Labate, C.A., 2016. Integrated analysis of gene expression from carbon metabolism, proteome and metabolome, reveals altered primary metabolism in Eucalyptus grandis bark, in response to seasonal variation. BMC Plant Biol. 16, 149. https://doi.org/10.1186/s12870-016-0839-8.

Carrillo, I., Mendonça, R.T., Ago, M., Rojas, O.J., 2018. Comparative study of cellulosic components isolated from different Eucalyptus species. Cellulose 25, 1011–1029. https://doi.org/10.1007/s10570-018-1653-2.

Chadni, M., Grimi, N., Bals, O., Ziegler-Devin, I., Brosse, N., 2019. Steam explosion process for the selective extraction of hemicelluloses polymers from spruce sawdust. Ind. Crops Prod. 141, 111757 https:// doi. org/ 10. 1016/j.indcr op. 2019. 111757.

Chen, H., Liu, J., Chang, X., Chen, D., Xue, Y., Liu, P., Lin, H., Han, S., 2017. A review on the pretreatment of lignocellulose for high-value chemicals. Fuel Process. Technol. 160, 196–206. https://doi.org/10.1016/j.fuproc.2016.12.007.

Evtuguin, D.V., Neto, C.P., Silva, A.M.S., Domingues, P.M., Amado, F.M.L., Robert, D., Faix, O., 2001. Comprehensive study on the chemical structure of dioxane lignin from plantation *Eucalyptus globulus* wood. J. Agric. Food Chem. 49, 4252–4261. https://doi.org/10.1021/jf010315d.

Feng, S., Cheng, S., Yuan, Z., Leitch, M., Xu, C., 2013. Valorization of bark for chemicals and materials: a review. Renew. Sustain. Energy Rev. 26, 560–578. https://doi.org/10.1016/j.rser.2013.06.024.

Fernandes, A., Cruz-Lopes, L., Dulyanska, Y., Domingos, I., Ferreira, J., Evtuguin, D., Esteves, B., 2022. Eco valorization of *Eucalyptus globulus* bark and branches through liquefaction. Appl. Sci. 12, 3775. https://doi.org/10.3390/app12083775.

Fernandes, M.C., Ferro, M.D., Paulino, A.F.C., Mendes, J.A.S., Gravitis, J., Evtuguin, D. V., Xavier, A.M.R.B., 2015. Enzymatic saccharification and bioethanol production from *Cynara cardunculus* pretreated by steam explosion. Bioresour. Technol. 186, 309–315. https://doi.org/10.1016/j.biortech.2015.03.037.

Foody, P., 1984. US Patent 4461648. Method for increasing the accessibility of cellulose in lignocellulosic materials, particularly hardwoods agricultural residues and the like,. https://doi.org/10.1016/0734–9750(84)90185-x.

Galletti, G.C., Reeves, J.B., 1992. Pyrolysis/gas chromatography/ion-trap detection of polyphenols (vegetable tannins): preliminary results. Org. Mass Spectrom. 27, 226–230. https://doi.org/10.1002/oms.1210270313.

Gao, H., Wang, Y., Yang, Q., Peng, H., Yuqi Li, Y., Zhan, D., Wei, H., Haiwen Lu, H., Bakr, M.M.A., EI-Sheekh, M.M., Qi, Z., Peng, L., Lin, X., 2021. Combined steam explosion and optimized green-liquor pretreatments are effective for complete saccharification to maximize bioethanolproduction by reducing lignocellulose recalcitrance in one-year-old bamboo. Renew. Energy 175, 1069–1079. https://doi.org/10.1016/j.renene.2021.05.016.

Gao, X., Laskar, D.D., Zeng, J., Helms, G.L., Chen, S., 2015. A 13C CP/MAS-based nondegradative method for lignin content analysis. ACS Sustain. Chem. Eng. 3, 153–162. https://doi.org/10.1021/sc500628s.

Gautam, R., Vanga, S., Ariese, F., Umapathy, S., 2015. Review of multidimensional data processing approaches for Raman and infrared spectroscopy. EPJ Tech. Instrum. 2, 8. https://doi.org/10.1140/epjti/s40485-015-0018-6.

Gilardi, G., Abis, L., Cass, A.E.G., 1995. Carbon-13 CP/MAS solid-state NMR and FT-IR spectroscopy of wood cell wall biodegradation. Enzym. Microb. Technol. 17, 268–275. https://doi.org/10.1016/0141-0229(94)00019-N.

Gominho, J., Costa, R.A., Lourenço, A., Quilhó, T., Pereira, H., 2021. *Eucalyptus globulus* stumps bark: chemical and anatomical characterization under a valorisation perspective. Waste Biomass Valoriz. 12, 1253–1265. https://doi.org/10.1007/s12649-020-01098-y.

Hawkes, G.E., Smith, C.Z., Utley, J.H.P., Vargas, R.R., Viertler, H., 1993. A comparison of solution and solid state ^{13}C NMR spectra of lignins and lignin model compounds. Holzforschung 47, 302–312. https://doi.org/10.1515/hfsg.1993.47.4.302.

Hemmingson, J.A., 1987. Steam-explosion lignins: Fractionation, composition, structure and extractives. J. Wood Chem. Technol. 7, 527–553. https://doi.org/10.1080/02773818708085284.

Hergert, H.L., 1971. Infrared spectra. In: Sarkanen, K.V., Ludwig, C.H. (Eds.), Lignins: Occurrence, Formation, Structure and Reactions. John Wiley & Sons, Inc, New York, pp. 267–297.

Horn, S.J., Eijsink, V.G.H., 2010. Enzymatic hydrolysis of steam-exploded hardwood using short processing time. Biosci. Biotechnol. Biochem. 74 (6), 1157–1163. https://doi.org/10.1271/bbb.90762.

Ibitoye, S.E., Jen, T.C., Mahamood, R.M., Akinlabi, E.T., 2021. Densification of agro-residues for sustainable energy generation: an overview. Bioresour. Bioprocess. 8, 75. https://doi.org/10.1186/s40643-021-00427-w.

Jacquet, N., Maniet, G., Vanderghem, C., Delvigne, F., Richel, A., 2015. Application of steam explosion as pretreatment on lignocellulosic material: a review. Ind. Eng. Chem. Res. 54, 2593–2598. https://doi.org/10.1021/ie503151g.

Kim, J., Lee, I., Yun, B., Chung, S., Shim, G., Koshino, H., Yoo, I., 2001. Ellagic acid rhamnosides from the stem bark of *Eucalyptus globulus*. Phytochemistry 57, 587–591. https://doi.org/10.1016/S0031-9422(01)00146-7.

Li, W.C., Han, L.J., Peng, T.B., Xie, Y.Y., Zou, Y., Li, L.Z., Jia, S.R., Zhong, C., 2020. Structural and behavior changes of herbaceous and hardwood biomass during steam explosion pretreatment and enzymatic hydrolysis. BioResources 15, 691–705. https://doi.org/10.15376/biores.15.1.691-705.

Liitiä, T., Maunu, S.L., Hortling, B., 2000. Solid state NMR studies on cellulose crystallinity in fines and bulk fibres separated from refined kraft pulp. Holzforschung 54, 618–624. https://doi.org/10.1515/hf.2000.104.

Lima, L., Miranda, I., Knapic, S., Quilhó, T., Pereira, H., 2018. Chemical and anatomical characterization, and antioxidant properties of barks from 11 *Eucalyptus* species. Eur. J. Wood Wood Prod. 76, 783–792. https://doi.org/10.1007/s00107-017-1247-y.

Lisbona, P., Pascual, S., Pérez, V., 2023. Waste to energy: trends and perspectives. Chem. Eng. J. Adv. 14, 100494 https://doi.org/10.1016/j.ceja.2023.100494.

Lourenço, A., Araújo, S., Gominho, J., Evtuguin, D., 2020. Cellulose structural changes during mild torrefaction of *Eucalyptus* wood. Polymers 12, 1–17. https://doi.org/10.3390/polym12122831.

Magina, S., Mendes, I.S.F., Prates, A., Evtuguin, D.V., 2022. Changes in sulfite liquor composition while re-profiling mill from paper-grade to dissolving pulp production. J. Wood Chem. Technol. 42, 193–203. https://doi.org/10.1080/02773813.2022.2068603.

Mason, W.H., 1926. US Patent 1578609. Process and apparatus for disintegration of wood and the like, Priority date Mar. 30 1926.

Miranda, I., Gominho, J., Pereira, H., 2012. Incorporation of bark and tops in *Eucalyptus globulus* wood pulping. BioResources 7, 4350–4361. https://doi.org/10.15376/biores.7.3.4350-4361.

Miranda, I., Gominho, J., Pereira, H., 2015. Heartwood, sapwood and bark variation in coppiced *Eucalyptus globulus* trees in 2nd rotation and comparison with the single-stem 1st rotation. Silva Fenn. 49, 1141. https://doi.org/10.14214/sf.1141.

Montipo, S., Ballesteros, I., Martins, A.F., Ballesteros, M., Camassola, M, Marli, 2020. Optimisation of uncatalysed steam explosion of lignocellulosicbiomasses to obtain Both C6- and C5-sugars. Wast Biomass-.-. Valor 11, 231–244. https://doi.org/10.1007/s12649-018-0396-5.

Nader, S., Brosse, N., Khadraoui, M., Fuentealba, C., Ziegler-Devin, I., Quilès, F., El-Kirat-Chatel, S., Mauret, E., 2022. A low-cost environmentally friendly approach to isolate lignin containing micro and nanofibrillated cellulose from *Eucalyptus globulus* bark by steam explosion. Cellulose 29, 5593–5607. https://doi.org/10.1007/s10570-022-04632-4.

Neiva, D., Fernandes, L., Araújo, S., Lourenço, A., Gominho, J., Simões, R., Pereira, H., 2015. Chemical composition and kraft pulping potential of 12 eucalypt species. Ind. Crops Prod. 66, 389–395. https://doi.org/10.1016/j.indcrop.2014.12.016.

Neiva, D.M., Araújo, S., Gominho, J., Carneiro, A. de C., Pereira, H., 2018. Potential of *Eucalyptus globulus* industrial bark as a biorefinery feedstock: chemical and fuel characterization. Ind. Crop. Prod. 123, 262–270. https://doi.org/10.1016/j.indcrop.2018.06.070.

Newman, R.H., 2004. Homogeneity in cellulose crystallinity between sam*ples of Pinus radiata* wood. Holzforschung 58, 91–96. https://doi.org/10.1515/HF.2004.012.

Obame, S.N., Ziegler-Devin, I., Safou-Tchima, R., Brosse, N., 2019. Homolytic and heterolytic cleavage of β-ether linkages in hardwood lignin by steam explosion. J. Agric. Food Chem. 67, 5989–5996. https://doi.org/10.1021/acs.jafc.9b01744.

Park, S., Baker, J.O., Himmel, M.E., Parilla, P.A., Johnson, D.K., 2010. Cellulose crystallinity index: measurement techniques and their impact on interpreting cellulase performance. Biotechnol. Biofuels 3, 10. https://doi.org/10.1186/1754-6834-3-10.

Ping, L., Brosse, N., Sannigrahi, P., Ragauskas, A., 2011. Evaluation of grape stalks as a bioresource. Ind. Crops Prod. 33, 200–204. https://doi.org/10.1016/j.indcrop.2010.10.009.

Prozil, S.O., Evtuguin, D.V., Lopes, L.P.C., 2012. Chemical composition of grape stalks of *Vitis vinifera* L. from red grape pomaces. Ind. Crops Prod. 35, 178–184. https://doi.org/10.1016/j.indcrop.2011.06.035.

Prozil, S.O., Evtuguin, D.V., Silva, A.M.S., Lopes, L.P.C., 2014. Structural characterization of lignin from grape stalks (*Vitis vinifera* L. J. Agric. Food Chem. 62, 5420–5428. https://doi.org/10.1021/jf502267s.

Quilhó, T., Pereira, H., Richter, H.G., 1999. Variability of bark structure in plantation-grown *Eucalyptus globulus*. IAWA J. 20, 171–180. https://doi.org/10.1163/22941932-90000677.

Rachocki, A., Pogorzelec-Glaser, K., Pietraszko, A., Tritt-Goc, J., 2008. The structural dynamics in the proton-conducting imidazolium oxalate. J. Phys. Condens. Matter 20, 505101. https://doi.org/10.1088/0953-8984/20/50/505101.

Ralph, J., Hatfield, R.D., 1991. Pyrolysis-Gc-Ms characterization of forage materials. J. Agric. Food Chem. 39, 1426–1437. https://doi.org/10.1021/jf00008a014.

Rebuzzi, F., Evtuguin, D.V., 2005. Effect of glucuronoxylan on the hornification of *Eucalyptus globulus* bleached pulps. Macromol. Symp. 232, 121–128. https://doi.org/10.1002/masy.200551414.

Santos, S.A.O., José, J., Freire, C.S.R., Domingues, M.R.M., Pascoal, C., Silvestre, A.J.D., 2012. Phenolic composition and antioxidant activity of Eucalyptus grandis, E. urograndis (*E. grandis* × *E. urophylla*) and *E. maidenii* bark extracts. Ind. Crop. Prod. 39, 120–127. https://doi.org/10.1016/j.indcrop.2012.02.003.

Sarker, T.R., Pattnaik, F., Nanda, S., Dalai, A.K., Meda, V., Naik, S., 2021. Hydrothermal pretreatment technologies for lignocellulosic biomass: a review of steam explosion and subcritical water hydrolysis. Chemosphere 284, 131372. https://doi.org/10.1016/j.chemosphere.2021.131372.

Segal, L., Creely, J.J., Martin, A.E., Conrad, C.M., 1959. An empirical method for estimating the degree of crystallinity of native cellulose Using the X-ray diffractometer. Text. Res. J. 29, 786–794. https://doi.org/10.1177/004051755902901003.

Selvendran, R.R., March, J.F., Ring, S.G., 1979. Determination of aldoses and uranic of vegetable fiber acid content. Anal. Biochem. 96, 282–292. https://doi.org/10.1016/0003-2697(79)90583-9.

Tanahashi, M., 1990. Characterization and degradation mechanisms of wood components by steam explosion and utilization of exploded wood. Bull. Wood Res. Inst. Kyoto Univ. 77, 49–117.

Trouvé, G., Michelin, L., Kehrli, D., Josien, L., Rigolet, S., Lebeau, B., Gieré, R., 2023. The multi-analytical characterization of calcium oxalate phytolith crystals from grapevine after treatment with calcination. Crystals 13, 967. https://doi.org/10.3390/cryst13060967.

Truong, Q., Koch, K., Yoon, J.M., Everard, J.D., Shanks, J.V., 2013. Influence of carbon to nitrogen ratios on soybean somatic embryo (cv. Jack) growth and composition. J. Exp. Bot. 64, 2985–2995. https://doi.org/10.1093/jxb/ert138.

Vale, M., Mateus, M.M., Galhano dos Santos, R., Nieto de Castro, C., de Schrijver, A., Bordado, J.C., Marques, A.C., 2019. Replacement of petroleum-derived diols by sustainable biopolyols in one component polyurethane foams. J. Clean. Prod. 212, 1036–1043. https://doi.org/10.1016/j.jclepro.2018.12.088.

Viola, E., Mariangela Cardinale, M., Santarcangelo, R., Villone, A., Zimbardi, F., 2008. Ethanol from eel grass via steam explosion and enzymatic hydrolysis. Biomass-.-. Bioenergy 32, 613–618. https://doi.org/10.1016/j.biombioe.2007.12.009.

Wang, Y., Lui, P., Zhang, G., Yang, Q., Lu, J., Xia, T., Peng, L., Wang, Y., 2021. Cascading of engineered bioenergy plants and fungi sustainable forlow-cost bioethanol and high-value biomaterials under green-like biomass processing. Renew. Sustain. Energy Rev. 137, 110586 https://doi.org/10.1016/j.sres.2020.110586.

Wyman, C.E., 1994. Ethanol from lignocellulosic biomass: technology, economics, and opportunities. Bioresour. Technol. 50, 3–15. https://doi.org/10.1016/0960-8524(94)90214-3.

Zhang, R., Gao, H., Wang, Y., He, B., Lu, J., Zhu, W., Peng, L., Wang, Y., 2023a. Challenges and perspectives of green-like lignocellulose pretreatments selectable for low-cost biofuels and high-value bioproduction. Bioresour. Technol. 369, 12831. https://doi.org/10.1016/j.biortech.2022.128315.

Zhang, R., Hu, J., Wang, Y., Hu, H., Li, F., Li, M., Ragauskas, A., Xia, T., Han, H., Tang, J., Yu, H., Xu, B., Peng, L., 2023b. Single-molecular insights into the breakpoint of cellulose nanofibers assembly during saccharification. Natur. Commun. 14, 1100. https://doi.org/10.1038/s41467-023-36856-8.

Zhu, J.Y., Pan, X.J., 2010. Woody biomass pretreatment for cellulosic ethanol production: Technology and energy consumption evaluation. Bioresour. Technol. 101, 4992–5002. https://doi.org/10.1016/j.biortech.2009.11.007.